Numerical Study of Solar Chimney with Absorber at Different Locations

Asst. Prof. Dr.Karima E. Amori **Asst. Lect. Khawla Naeem Hmood**
Univ. of Baghdad/ Mech. Eng. Dept. , Aljaderiya - Baghdad-Iraq
drkarimaa@yahoo.com nh.khawla@yahoo.com

ABSTRACT:
Heat transfer process and fluid flow in a solar chimney used for natural ventilation are investigated numerically in the present work. Solar chimney was tested by selecting different positions of absorber namely: at the back side, front side, and at the middle of the air gap. CFD analysis based on finite volume method is used to predict the thermal performance, and air flow in two dimensional solar chimney under unsteady state condition, to identify the effect of different parameters such as solar radiation. Results show that a solar chimney with absorber at the middle of the air gap gives better ventilation performance. A comparison between the numerical and previous experimental results shows fair agreement.

Key Words: solar chimney, CFD, buoyancy; natural ventilation; free cooling

دراسة نظرية لمدخنة شمسية لمواقع مختلفة للسطح الماص

أ.م.د. كريمة أسماعيل عموري م.م. خولة نعيم حمود
جامعة بغداد- كلية الهندسة – قسم الميكانيك

الخلاصه

تم إجراء درسة عددية لعملية انتقال الحرارة وجريان المائع في المدخنة الشمسية. اختبرت المدخنة الشمسية بأختيار مواقع مختلفة للسطح الماص وتحديدا" بوضع السطح الماص على الجانب الخلفي ، الجانب الأمامي ، وفي منتصف فجوة الهواء. تم استخدام تحليل ديناميك الموائع الحسابية وبأعتماد طريقة الحجوم المحددة لتحديد الأداء الحراري وجريان الهواء في مدخنة شمسية ببعدين ولظروف غير مستقرة لبيان تأثير عوامل مختلفة مثل الأشعاع الشمسي. بينت النتائج ان المدخنة الشمسية بسطح ماص في منتصف الفجوة الهوائية يؤدي افضل تهوية . بينت المقارنة بين النتائج الحالية والنتائج التجريبية السابقة توافقا مقبولا".

الكلمات الرئيسية: مدخنة شمسية ، ديناميك الموائع الحسابية ، الطفو ، التهوية الطبيعية ، التبريد الغير مكلف.

INTRODUCTION

A solar chimney (or thermal chimney) is a way for improving the natural ventilation of buildings by using convection of air heated by passive solar energy. Passive solar design refers to the use of the sun's energy for heating and cooling of living spaces. Operable windows, thermal mass and solar chimneys are common elements found in passive design. **Bouchair and Fitzgerald (1988)** conducted a theoretical study of the heat stored in solar chimney using a finite difference technique. They showed that the amount of the heat collected is strongly dependent upon its azimuth. **Bansal et al.(1989)** used a mathematical model to calculate the performance of a wind tower system integrated with a solar chimney. The work aimed to predict the results based on the proposed energy balance equation of the solar chimney and air flow rate equations. The study also confirmed that the thermal performance of the solar chimney was comparatively higher for lower incident winds. The result showed that the solar chimney can increase the mass flow rate of induced air by up to 50% for the case of high incident solar radiation and low wind speeds. The solar chimney integrated with a wind tower was able to generate airflow up to 1.4 kg/s which doubles that of a single wind tower producing only up to 0.75 kg/s. The author concluded that the effect of the solar system is more significant than that of the wind tower and combining both systems will enhance the ventilation rates by increasing the mass flow rate of induced air. **Awbi and Gan(1992)** compared the analytical and simulated solution for Trombe wall and solar chimney. Air speed and temperature results showed that airflow within the solar chimney ducts was not symmetrical due to air entering at right angle to the duct. **Ong(2003)** proposed a simple mathematical model of a solar chimney. The physical model is similar to that of the Trombe wall. The equations were solved using a matrix-inversion solution procedure. The thermal performance of the solar chimney as determined from the glass, wall and air temperatures, air mass flow rate and instantaneous heat collection efficiency of the chimney are presented. Satisfactory correlation was obtained with experimental data from other investigators. Later, **Ong and Chow (2003)** proposed a mathematical model of a solar chimney to predict its performance under varying ambient and geometrical features. Steady state heat transfer equations were set up using a thermal resistance network and solved using matrix inversion. The effects of air gap and solar radiation intensity on the performance of different chimneys were investigated.

Chantawong et al. (2006) studied the thermal performance of Glazed Solar Chimney Walls (GSCW) under the tropical climatic conditions of Thailand. A prototype of GSCW was integrated into southern wall of a small room of 2.8m³ volume . They found that GSCW is highly suitable for hot countries, it can reduce heat gain through glass walls into the house by developing air circulation, which can help improve the thermal comfort of residents too. The use of GSCW can also reduce the usage of fans due to induced ventilation. **Mathur et.al (2006)** investigated experimentally the effect of the ratio between height of absorber and air gap of a solar chimney used for room ventilation. They found that highest rate of ventilation induced with the help of solar energy was 5.6 air changes per hour in a room of (27 m^3), at solar radiation 700 W/m^2 incident on vertical surface with the height to air gap ratio of 2.83. **Jia et.al. (2007)** presented a mathematical model for simulating air flow within solar channel of the insulated Trombe solar wall system. They discretized and solved mass, momentum and energy conservation equations using the finite difference method. They carried out experimental study of solar chimney to validate the proposed mathematical model. The differences between the predicted and measured results of airflow rate were less than 3%. **Harris and Helwig (2007)** studied numerically the design of a solar chimney to induce ventilation in building. CFD modeling was used to assess the impacts of inclination

angle, double glazing and low-emissivity finishes on the induced ventilation rate. A solar chimney south facing chimney of dimensions (3m) height, (0.1-0.3m) cavity width, and (1m) cavity breadth, at an inclination angle of 67.5^{o} from the horizontal for the location chosen (lat. 52^{o}on 15^{th} July), gives 11% greater efficiency than the vertical chimney, and a 10 % higher efficiency was obtained by using a low – emissivity wall surface. **Lee and Strand(2009)** used numerical simulation and found that: (1) chimney height, solar absorptance and solar transmittance turned out to have more influences on natural ventilation improvement than air gap width.

Kaiser and Zamora (2009) have studied numerically the laminar and turbulent flow induced by natural convection in channels. Numerical results of the average Nusselt number and the non- dimensional induced mass-flow rate have been obtained for values of Rayleigh number varying from 10^{5} to 10^{12} for symmetrical and isothermal heating. **Gan(2010)** used CFD to simulate the natural ventilation of buildings using two different sizes of computational domain for different heat fluxes and wall heat distribution. He found that utilizing computational domain larger than the physical size gives accurate prediction of the flow rate and heat transfer in ventilated buildings with large openings, particularly with multiple inlets and outlets as demonstrated with two examples for natural ventilation of buildings. **Rahimi and Bayat** (2011) investigated a buoyancy induced air flow within a vertical pipe experimentally. The flow rate was a function of the pipe height, surrounding temperature and mean temperature of air inside the pipe. They found that the pressure losses at the inlet and outlet of the pipe along with that of the main pipe are compensated by the buoyancy pressure. The flow rate increases as the length of the pipe is increased and its variation becomes negligible for extremely large length of pipe. For a constant length of the pipe, the maximum of flow rate occurs where the mean temperature of the flow is one and a half times greater than the surroundings temperature.

Tan and Wong (2012) constructed a solar chimney system to enhance the air ventilation within the interior spaces using a series of solar assisted ducts that linked the lower floor classrooms and upper floor hall in a zero energy building (three story building) in Singapore. Results showed that the solar chimney system is operating well in the hot and humid tropics, including cooler days. The interconnecting thermal stack experienced in the hall, can induce an average air speed of 1.5 m/s and 0.4 m/s within the solar chimney and level 1 classroom respectively.

The objective of the present work is to investigate numerically the thermo-fluid phenomena takes place in a full scale solar chimney under Iraq environmental condition testing different positions of the absorber (at front side, back side, and at the middle of the air gap) which is up to date is rarely studied.

MATHEMATICAL MODEL

A mathematical model of the natural buoyancy-driven fluid flow and heat transfer in the chimney shown in Figure(1) have been adopted. The following assumptions have been used to simplify the governing equations:

1- Transient incompressible 2-D air flow in the chimney (no variations are considered along the width).
2-Conduction heat transfer along the absorber wall and the glass cover is neglected
3- Radiation heat transfer is neglected.
4- Constant thermo-physical properties of the working fluid.
5- Air density is dependent of temperature.
6- Dissipation Function is neglected.

Governing Equations

The governing differential equations of the natural convection in the solar chimney may be written in Cartesian coordinates as: (**Versteeg and Lasekea 1995**)

Continuity equation:

$$\frac{\partial \rho}{\partial t}+\frac{\partial}{\partial x}(\rho u)+\frac{\partial}{\partial y}(\rho v)=0 \quad (1)$$

X-momentum equation:

$$\frac{\partial}{\partial t}(\rho u)+\frac{\partial}{\partial x}(\rho uu)+\frac{\partial}{\partial y}(\rho vu)= -\frac{\partial P}{\partial x}+\frac{\partial}{\partial x}(\mu\frac{\partial u}{\partial x})+\frac{\partial}{\partial y}(\mu\frac{\partial u}{\partial y}) -\rho g(T-T_\infty)\sin\theta \quad (2)$$

Y-momentum equation:

$$\frac{\partial}{\partial t}(\rho v)+\frac{\partial}{\partial x}(\rho uv)+\frac{\partial}{\partial y}(\rho vv)= -\frac{\partial P}{\partial y}+\frac{\partial}{\partial x}(\mu\frac{\partial v}{\partial x})+\frac{\partial}{\partial y}(\mu\frac{\partial v}{\partial y}) -\rho g(T-T_\infty)\cos\theta \quad (3)$$

Energy equation:

$$\frac{\partial}{\partial t}(\rho T)+\frac{\partial}{\partial x}(\rho uT)+\frac{\partial}{\partial Y}(\rho vT)= \frac{\partial}{\partial x}\left(\Gamma\frac{\partial T}{\partial x}\right)+\frac{\partial}{\partial y}\left(\Gamma\frac{\partial T}{\partial y}\right) \quad (4)$$

where:

$$\Gamma=\frac{\mu}{pr}$$

x, y Cartesian-coordinate of the system.

ρ & μ are air density (kg.m^{-3}) and dynamic viscosity (kg/m.s) respectively

For (Ra > 10^9) k- ε turbulence model is used, and μ, Γ are replaced by their effective values μ_{eff} which can be defined as sum of the eddy viscosity μ_t and fluid dynamic viscosity μ (**Andonikos et al.2007**). The turbulent kinetic energy and the dissipation rate can be defined using the following equations:

$$\frac{\partial}{\partial t}(\rho k)+\frac{\partial}{\partial x}(\rho uk)+\frac{\partial}{\partial y}(\rho vk)= \frac{\partial}{\partial x}\left(\Gamma_k\frac{\partial k}{\partial x}\right)+\frac{\partial}{\partial y}\left(\Gamma_k\frac{\partial k}{\partial y}\right)+S_k \quad (5)$$

where

$$\Gamma_k=\mu_{eff}/\delta_k \quad (6)$$

$$S_k=G-C_D\rho\varepsilon \quad (7)$$

$$\mu_t=\rho C_\mu k^2/\varepsilon \quad (8)$$

$$\frac{\partial}{\partial t}(\rho\varepsilon)+\frac{\partial}{\partial x}(\rho u\varepsilon)+\frac{\partial}{\partial y}(\rho v\varepsilon)= \frac{\partial}{\partial x}\left(\Gamma_\varepsilon\frac{\partial \varepsilon}{\partial x}\right)+\frac{\partial}{\partial y}\left(\Gamma_\varepsilon\frac{\partial \varepsilon}{\partial y}\right)+C_1\frac{\varepsilon}{k}G-C_2\rho\frac{\varepsilon^2}{k} \quad (9)$$

where

$$G=\mu_t\left(2\left[\left(\frac{\partial u}{\partial x}\right)^2+\left(\frac{\partial v}{\partial y}\right)^2\right]+\left(\frac{\partial u}{\partial y}+\frac{\partial v}{\partial x}\right)^2\right)$$

$$\Gamma_\varepsilon=\mu_{eff}/\delta_\varepsilon$$

The turbulent constants ($C_\mu, C_D, C_1, C_2, \delta_k$, and δ_ε) are given in table (1)

Boundary and Initial Conditions

The air velocity boundary conditions at inlet of the chimney are: **(Mossowi 2001)**

$$\mathbf{u(x,0)=0 \quad ; \quad v(x,0)=v_{in}} \quad (10)$$

While the inlet air temperature is:

$$\mathbf{T(x,0)=T_\infty}$$

The outlet boundary conditions can be written as: (**Kasayapanand 2007**)

$$\left.\frac{\partial u}{\partial y}\right|_L=\left.\frac{\partial v}{\partial y}\right|_L=0 \qquad \left.\frac{\partial T}{\partial y}\right|_L=0 \;;\; P(x,L)=P_\infty \quad (11)$$

No slip boundary conditions are adopted on solid boundaries

$$u(0,y)=v(0,y)=0 \qquad u(w,y)=v(w,y)=0 \quad (12)$$

The glass cover and absorber are subjected to the following thermal boundary conditions:

$$\frac{\partial T}{\partial x}(0,y)=\alpha_g I \;;\; \frac{\partial T}{\partial x}(w,y)=\tau\alpha I$$

respectively, where α_g is glass absorbtivity.

The turbulent kinetic energy and the dissipation rate at the inlet of the chimney are: (**Mosi and Clayton 1980**)

$$k(x,0)=k_{in}=C_k v_{in}^2 \qquad \varepsilon(x,0)=\varepsilon_{in}=C_\mu k_{in}^{3/2}/(0.5D_hC_\varepsilon) \quad (13)$$

where D_h is the hydraulic diameter.

while at the outlet (**Taylor et al. 1984**):

$$\left.\frac{\partial k}{\partial x}\right|_{y=L} = \left.\frac{\partial \varepsilon}{\partial x}\right|_{y=L} = 0 \qquad (14)$$

The boundary conditions for turbulent model (when $Ra > 10^9$ (**Patankar 1980**) are:

$$k(0,y) = \left.\frac{\partial \varepsilon}{\partial y}\right|_{y=0} = 0$$
$$k(w,y) = \left.\frac{\partial \varepsilon}{\partial y}\right|_{y=L} = 0 \qquad (15)$$

The following initial conditions used through the numerical solution can be written as:

$$T = T_\infty \;;\; P = P_\infty$$
$$u = v = 0 \quad (x,y,t=0) \qquad (16)$$

The above governing equations together with the boundary and initial conditions have been solved numerically using SIMPLE algorithm with segregated unsteady-state solver embodied in Fluent commercial software. The material and thermophysical properties needed are presented in table (2).

Figure (1) shows the different views for the investigated solar chimneys. The main parts of the solar chimney are the absorber wall, 2.25m height (ductile steel plate of 0.001m thickness), and the glass cover of (0.004m) thickness.

Air flow rate through the channel is calculated such that:

$$Q_{vent} = v_{avg} * A \qquad (17)$$

where:

v_{avg} is the average velocity at the exit cross section of the chimney (m/s)

A is the outlet cross section area of the chimney (0.1455 m^2)

Q_{vent} is the flow rate of the hot air (m^3/s).

The weather data such as (ambient temperature, solar radiation and wind speed) was adopted for Al-Kufa city located at (44.34° longitude East) and (32° latitude North) (**Mohammed 2010**) on 20th July 2010. The hourly average air velocity (V_{avg}) at chimneys outlet is calculated as:

$$V_{avg} = \frac{1}{W}\int_0^W V dx \qquad (18)$$

where:

W=thickness of air gap (m)

Air Change per Hour (ACH) refers to the amount of air ventilated and replaced by fresh air. This parameter can be calculated as:-

$$ACH = \frac{Q_{vent} \times 3600}{V} \qquad (19)$$

where V is the volume of a room taken as $(3 \times 4 \times 3)\ m^3$

The thermal efficiency of the solar chimney is calculated as:

$$\eta = \frac{\rho\, Q_{vent}\ Cp(T_{out} - T_{in})}{I \times L \times b} \qquad (20)$$

where:

η thermal efficiency

Cp air specific heat (J/kg K)

I incident solar energy (W/m^2).

L absorber height = 2.25m

b chimney's width =0.97m

Numerical Approach

The Navier–Stokes equations simultaneously with the continuity governing equations and energy equations together with the boundary and initial conditions have been solved numerically using SIMPLE algorithm with segregated unsteady-state solver embodied in Fluent commercial software.

RESULTS AND DISCUSSION

Testing the performance of the solar chimney was performed at ambient conditions on 20th July 2010 in Al-Najaf city (32.° lat north). Numerical experiments have been conducted on vertical solar chimney with absorber at the front side, at the back side , and at the middle of the air gap.

The hourly distribution of solar radiation (I) and ambient temperature (T_∞) are displayed in Figure(2). These values are

adopted as input data to the simulation code. The maximum incident solar radiation and ambient temperature were (945 W/m^2 and 47.7 ^oC) respectively.

The predicted absorber average temperature was compared with the measured values published by **Mohammed (2010)** as shown in Fig.(3). The minimum and maximum deviations were (0.44% and 18.83%) respectively.

Figure(4) shows the variation of hourly absorber temperature and glass cover temperature at five different levels (T1 to T5) along chimneys height which are given in table (4). These temperatures are changing along with the intensity of solar radiation. The highest maximum absorber temperature was (94.5 ^oC at 12:00 PM), while the glass cover temperature was (59.4 ^oC at 12:00 PM).

Figure (5) illustrate a comparison of absorber temperature between cases I and II. Higher absorber temperature is reported for case I since the absorber is back insulated, while air is in contact with the two faces of absorber for case II. The same results are obtained in Fig.(6).

Figure(7) shows the variation of hourly air average temperature at different heights along the chimney for case I. The maximum air temperature recorded is (77^oC). The maximum air temperature reported was (60^oC) for case II as shown in Fig. (8), while for case III it was (53^oC) for air gap between glass cover and absorber, and (54.5^oC) for air gap behind the absorber as depicted in Fig.(9).

A considerable change in air velocity of induced ventilation during day hours is shown in Fig.(10). The distribution of air velocity across the air gap for case III is presented in Fig.(11). The maximum air velocity is indicated near the absorber (before and after the absorber). Figure (12) reported higher values of air change per hour for case III compared with cases I and II, while its thermal efficiency was the lowest as shown in Fig.(13).

CONCLUSIONS

The effect of different locations of the absorber at thermal and air velocity inside a solar chimney used for induce natural ventilation has been studied numerically. The following conclusions can be extracted;

1) The position of absorber affects the performance of the chimney. Solar chimney with absorber at middle of air gap has the best thermal performance.
2) The thermal performance of the solar chimney is decreased when absorber is located at front side. Quantitatively the maximum air temperature reached at chimneys' outlet was (77^oC) for absorber at back side while it was (60 ^oC) when absorber at front side.
3) The highest air change per hour was obtained for solar chimney with absorber at the middle of air during day hours.
4) The highest thermal efficiency was indicated for solar chimney with absorber at the back side during day hours.

REFERENCES

Al Mossowi A.N., Turbulent developing flow and heat transfer in a porous square duct, MSc. Thesis, Mechanical and Construction Department, University of Technology, Baghdad, Iraq 2001, (written in Arabic)

Andronikos E.F., Dionysios M., Evngellos B., Michalis GR.V., Maria K.K., Stamatis A.M., Study of natural convection phenomena inside a wall solar chimney with one wall adiabatic and one wall under a heat flux, Applied thermal engineering 27 (2007) 2266-2275.

Awbi H.B., Gan G., Simulation of solar-induced ventilation, Renewable Energy Technology and the Environment 4 (1992) 2016–2030.

Bansal NK, Mathur R. Solar chimney for enhanced stack ventilation. Build Environ 28 (1989) 373–7.

Bassiouny R., Korah N.S.A., Effect of solar chimney inclination angle on space flow pattern and ventilation rate, Energy and Buildings 41 (2009) 190-196.

Bouchair A., Fitzgerald D., The optimum azimuth for a solar chimney in hot climates, Energy and Building 12 (1988) 135-140.

Chantawong P., Hirunlabh J., Zeghmati B., Khedari J., Teekasap S., Win M.M., Investigation on thermal performance of glazed solar chimney walls, Solar Energy, 80 (2006) 288-297.

Eckert E., Jackson T.W., Analysis of turbulent free convection boundary layer on flat plate, (Report 1015, (1950) supersedes NACA TN 2207).

Gan G., Simulation of buoyancy-driven natural ventilation of buildings-impact of computational domain, Energy and Building 42 (2010) 1290-1300.

Harris D.J., Helwig N., Solar chimney and building ventilation, Applied Energy 84 (2007) 135–146.

Jia H., Li J., Duanmu X., Li Y., Sun Y., Study on the air movement character in solar wall system, College of architecture and civil engineering, Beijing university of technology, (2007), Beijing, 100022 Building simulation.

Kaiser A.S, Zamora B., Optimum wall-to-wall spacing in solar chimney shaped channels in natural convection by numerical investigation, Applied thermal Eng. 29 (2009) 762–769.

Kasayapanand N., Enhanced heat transfer in inclined solar chimneys by electro-hydrodynamic technique, School of Energy, Environment, and Materials 1 (2007) 0960-1481.

Lee K.H., Strand .K., Enhancement of natural ventilation in buildings using a thermal chimney, Energy and Buildings 41 (2009) 615–621.

Mathur J., Bansal N.K, Mathur S., Anupma J.M., Experimental investigations on solar chimney for room ventilation, Solar Energy 80 (2006) 927–35.

Mohammed S.W., Experimental and numerical studies of solar chimney for natural ventilation in Iraq, MSc. thesis, Mechanical Eng. dept. , college of Eng., University of Baghdad, 2010.

Morsi Y.S., Clayton B. R., Determination of principal characteristics of turbulent swirling flow along annuli, Int. J. Heat and Fluid Flow 7 (1980) 208-222.

Ong K.S., A mathematical model of a solar chimney. Renewable Energy 28 (2003) 1047–60.

Ong K.S., Chow C.C., Performance of a solar chimney. Solar Energy 74 (2003) 1–17.

Patankar S.V., Numerical heat transfer and fluid flow, McGraw Hill, 1980, New York.

Rahimi M., Bayat M.M., An experimental study of naturally driven heated air flow in a vertical pipe, Energy and Buildings 43 (2011) 126-129.

Tan A.Y.K., Wong N.H., Natural ventilation performance of classroom with solar chimney system, Energy and Buildings 53 (2012) 19–27.

Taylor, Rance J., Medwell J.O., Turbulent flow and heat transfer in rotating ducts-preliminary results, Numerical methods for non-linear problems, Pincridge Press Swansea, U.K., 2 (1984) 839-847.

Versteeg H.K., Lasekera W. Mala, An introduction to computational fluid dynamics. The Finite Volume Method, 1st Pub., (1995) Long Man Group Ltd.

Table (1): Values of Constants Used in
the $(k-\varepsilon)$ Model (**Eckert and Jackson 1950)**

C_μ	C_D	C_1	C_2	δ_k	δ_ε
0.09	1.00	1.44	1.92	1.0	1.3

Table (2): Physical Properties Of Used Materials
(Ong and Chow2003, Mohammed2010)

material	ρ kg/m^3	Cp J/kg.^{o}C	k_t W/m.^{o}C	Emissivity ε_t	absorptivity α	transmisivity τ
Absorber (ductile steel)	7850	500	0.345	0.95	0.95	0
Cover (comm. Glass)	2470	750	1.0	0.9	0.06	0.84
Air	1.1614 - 3.53E-3(T-300)	1007 - 4E-3(T-300)	(263+0.74(T-300)E-4	**(Bassiouny and Korah 2009)**		

Table (3): Computed Average Outlet Velocity Results (V_{wind}=1 m/s)

Time (hr)	I solar glass	T amb	V_{out} Case I	V_{out} Case II	V_{out} Case III
10	824	41.2	1.204	1.136	1.274
11	927	43.4	1.242	1.171	1.365
12	945	45.3	1.244	1.172	1.466
13	921	46.8	1.228	1.156	1.331
14	838	47.3	1.199	1.119	1.313
15	673	47.6	1.155	1.0720	1.198
16	484	47.7	1.121	1.0723	1.145
17	275	47.5	1.117	1.031	1.133

Table (4): Locations of indicated temperatures

symbol	T1	T2	T3	T4	T5
Distance from inlet y= (mm)	260	755	1250	1745	2240

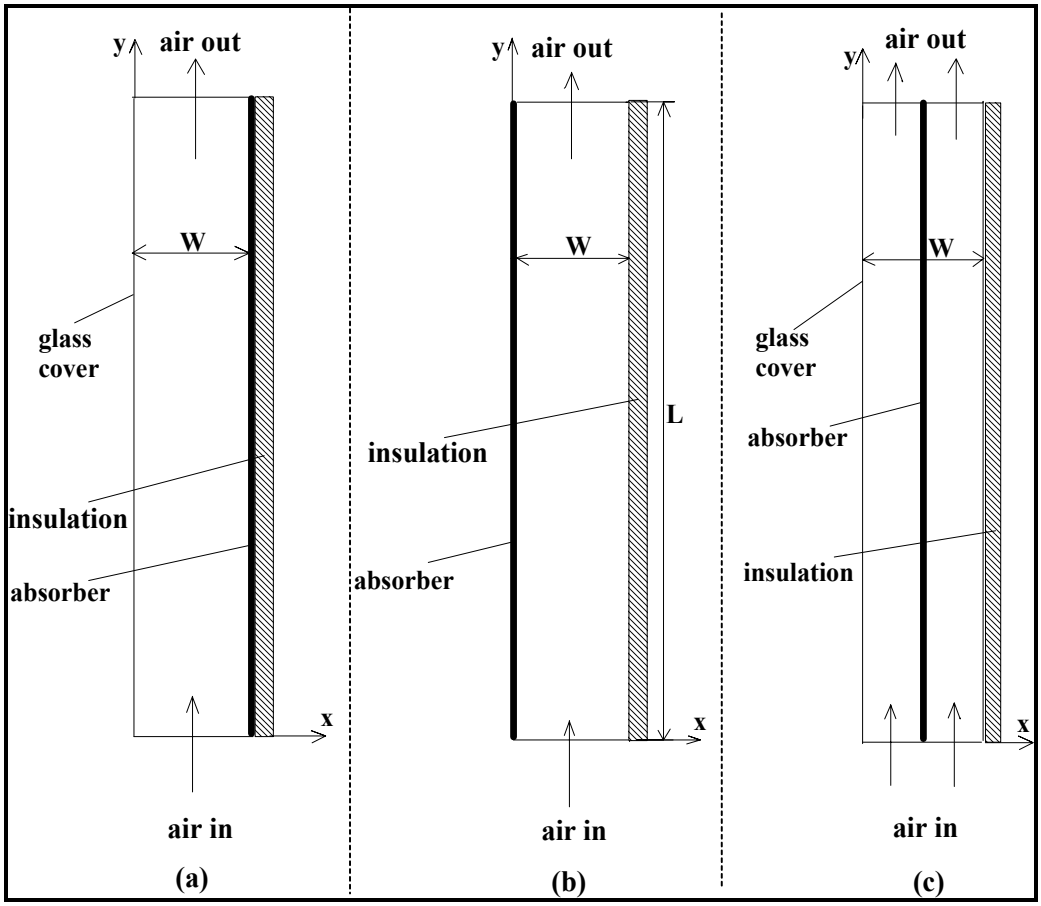

Fig.(1): Schematic Diagram of the Cases Studied of Solar Chimney. a) absorbe at back side, b) absorber at front side, c) absorber at the middle of air gap.

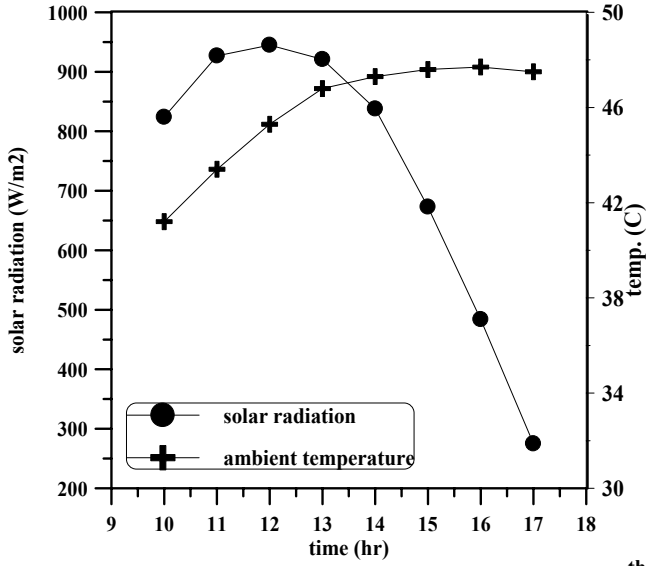

Fig.(2): Variation of Measured Ambient Conditions on 20th July 2010.

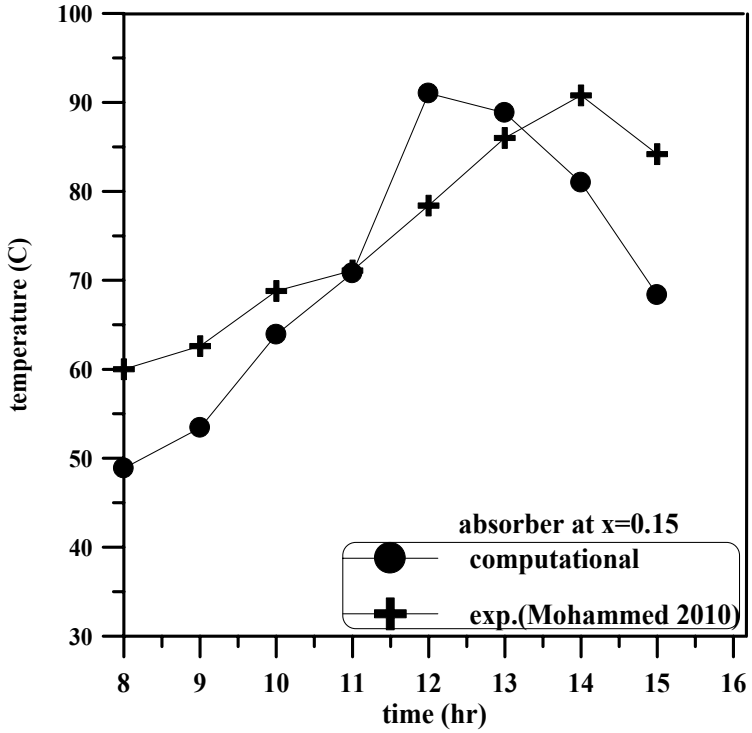

Fig.(3): Hourly Variation of Absorber Average Temperature. Comparison between the Computed results and Experimental results (Mohammed 2010)

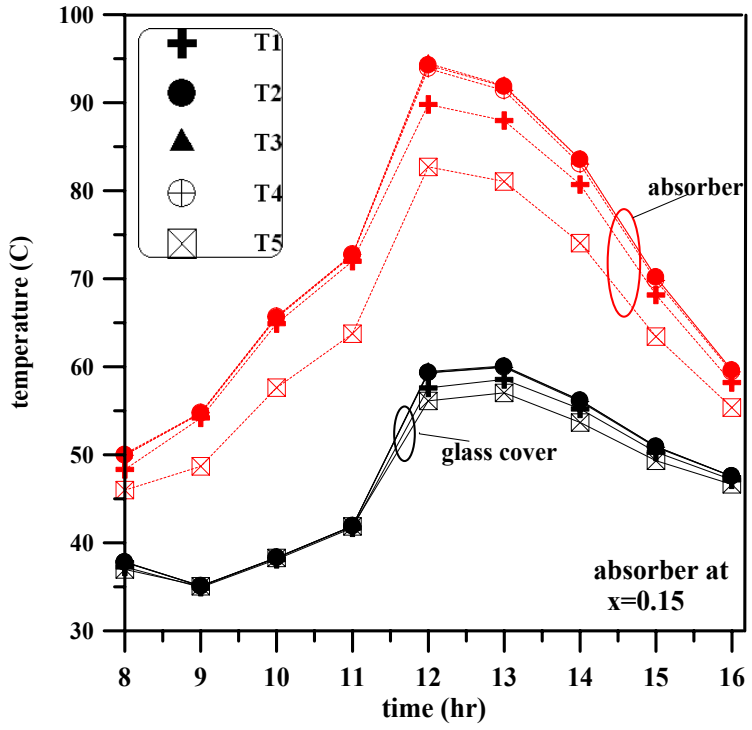

Fig. (4): Hourly Temperature distribution Case I

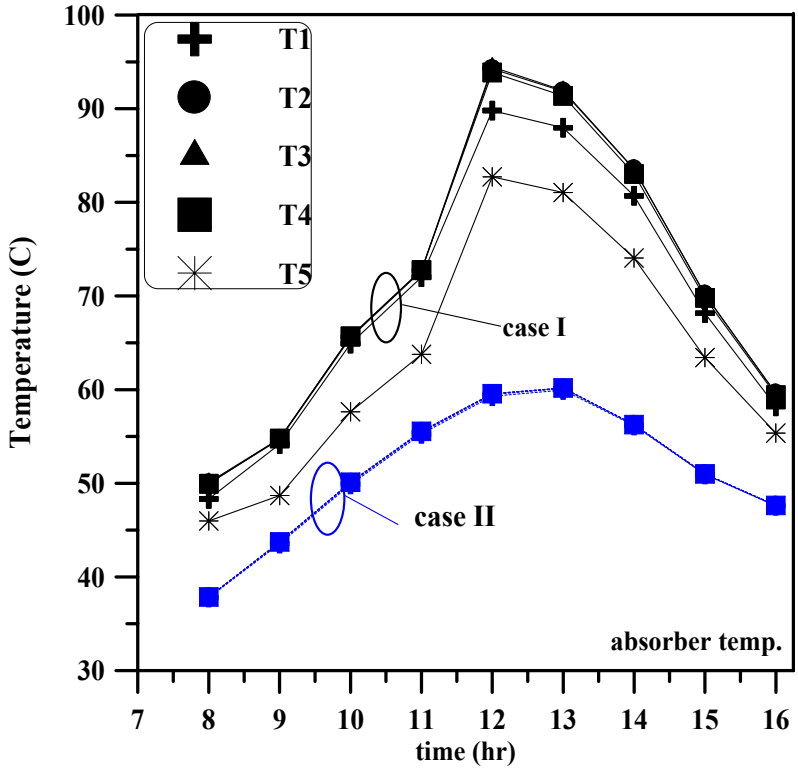

Fig. (5): Comparison of Hourly Temperature Distribution between Case I and Case II

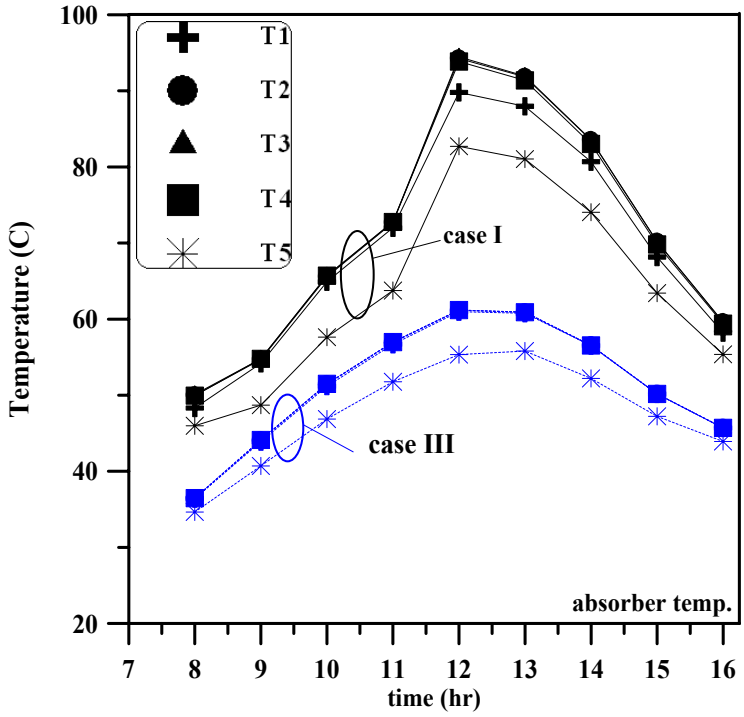

Fig.(6): Comparison of Hourly Temperature Distribution of the absorber between Case I and Case III

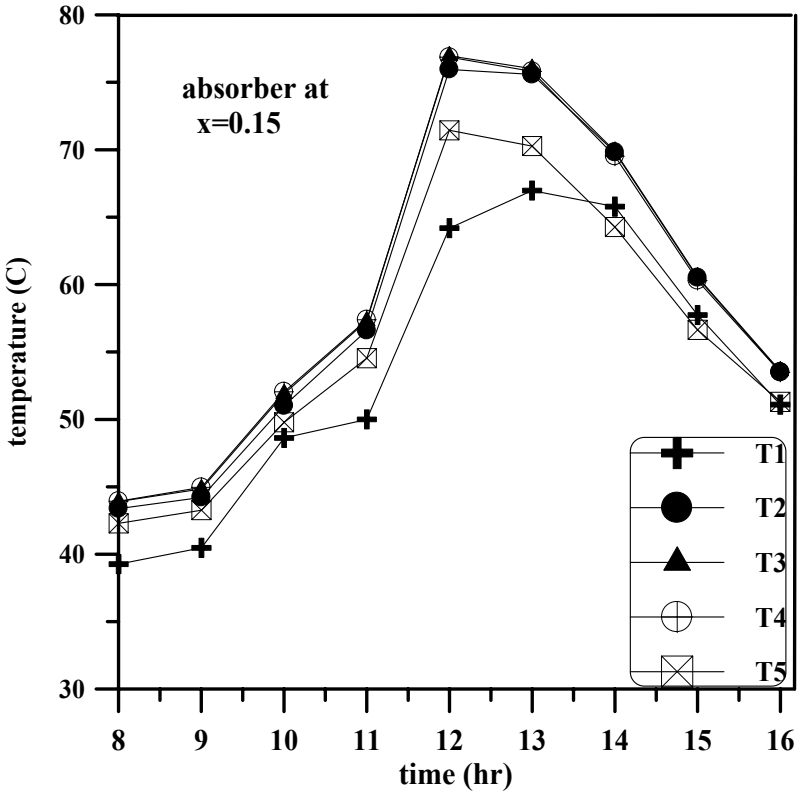

Fig.(7): Hourly air Temperature distribution inside the chimney Case I

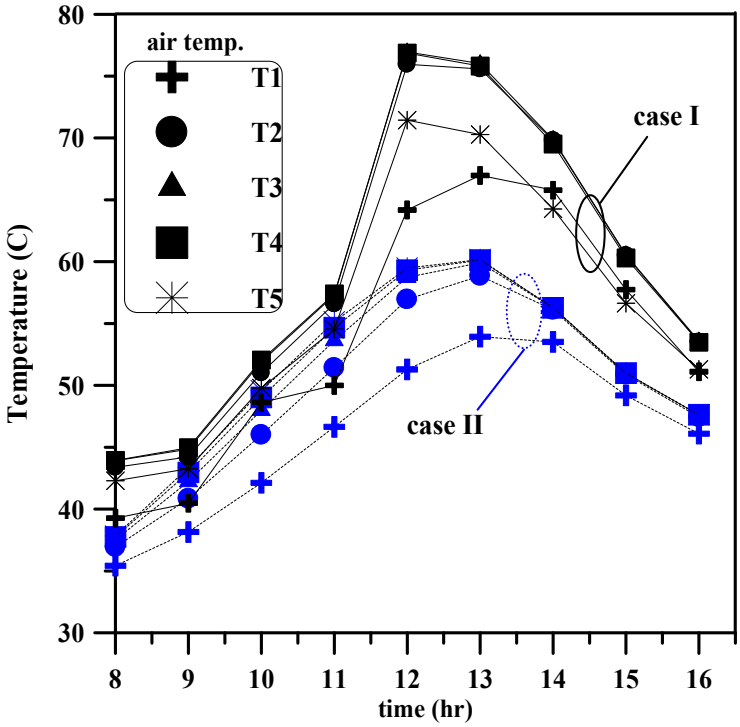

Fig.(8): Comparison of Hourly Air Temperature Distribution between Case I and Case II

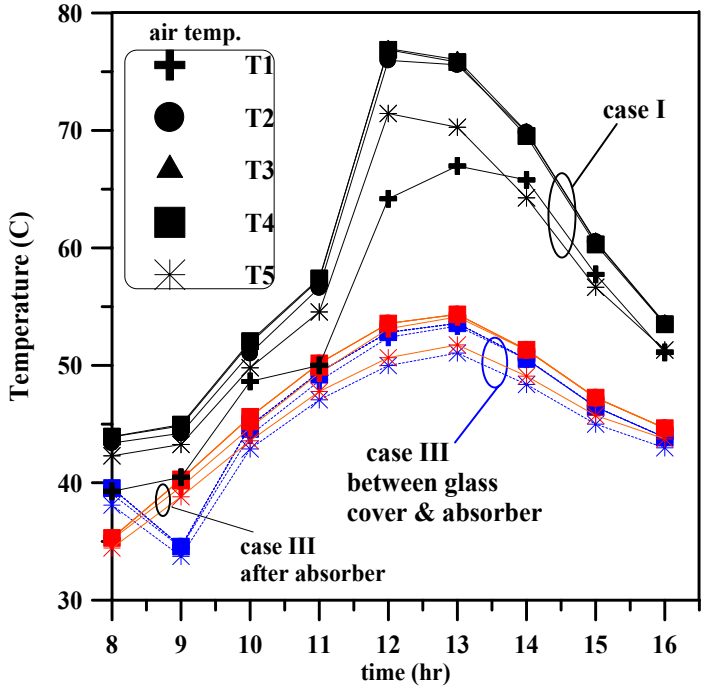

Fig. (9): Comparison of Hourly Air Temperature Distribution between Case I and Case III

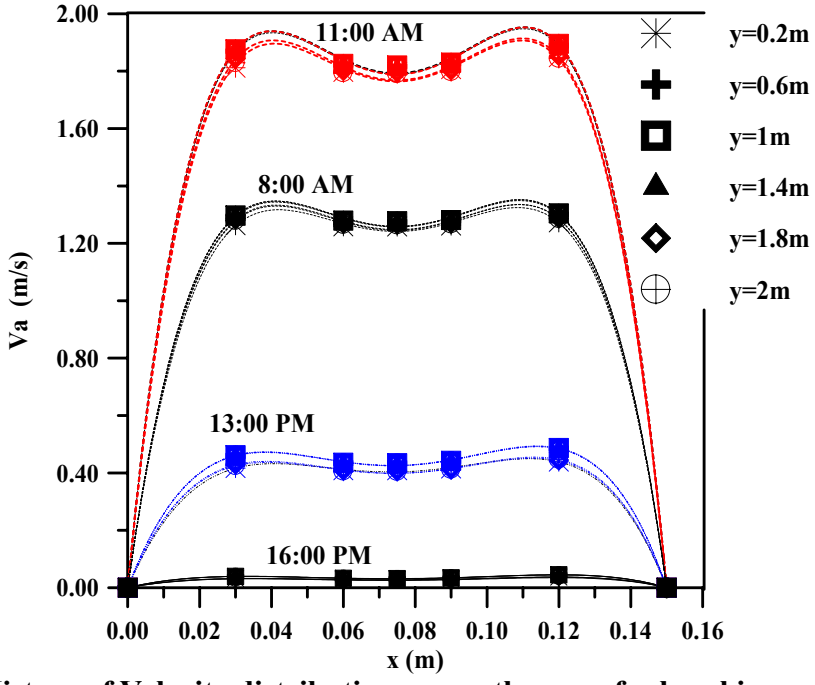

Fig.(10): History of Velocity distribution across the gap of solar chimney for case I

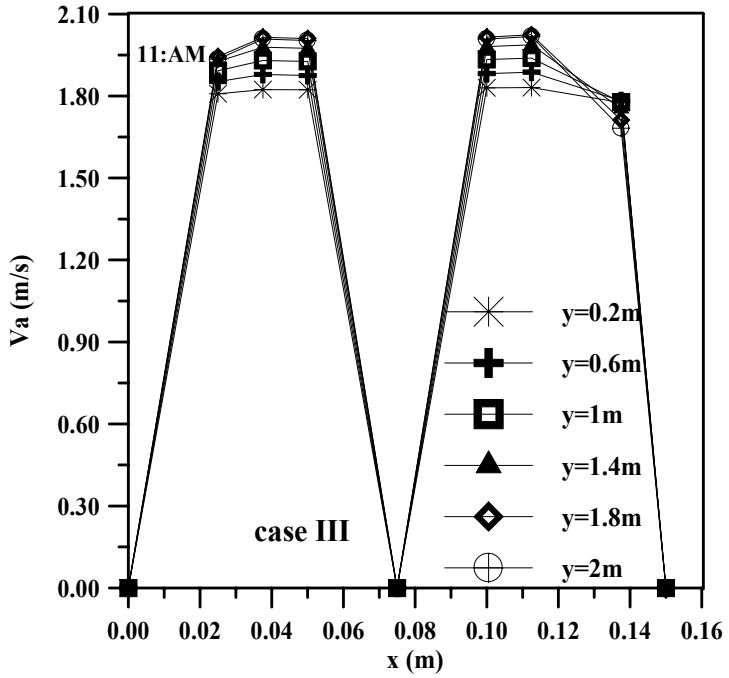

Fig.(11): History of Velocity distribution across the gap of solar chimney for case III

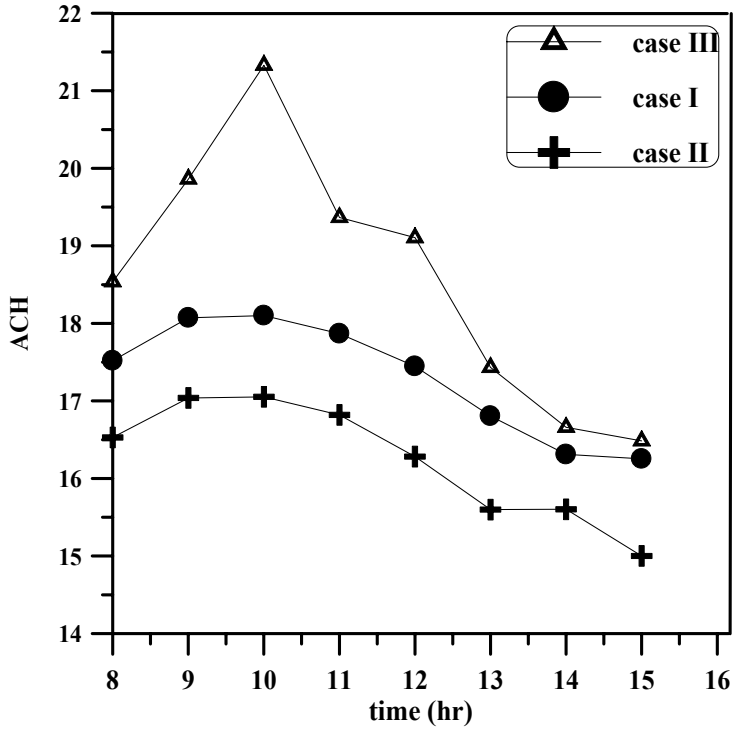

Fig.(12): History of Air Change per Hour of solar chimney

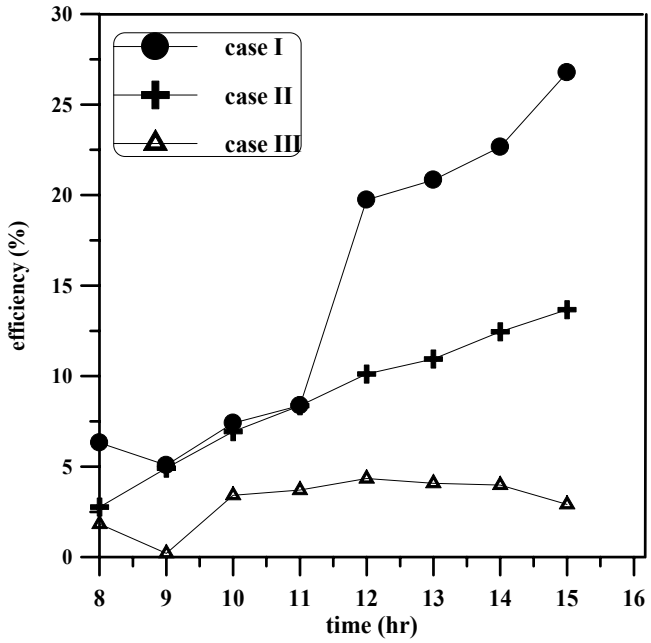

Fig.(13): History of solar chimneys efficiency.

Nomenclature

Latin Symbols			
A	surface area (m^2)	Q_{vent}	Air discharge (m^3/s)
D_h	Hydraulic diameter (m)	t	time (s)
C_P	Specific heat (J/kg. K)	$T\infty$	Ambient temperature (K)
g	gravitational acceleration(m/s^2) kinetic energy generation by shear (J)	$T_{i,m}$	Air inlet temperature (K)
h	heat transfer coefficient ($W/m^2.K$)	$T_{o,m}$	Air out temperature (K)
I	solar radiation (W/m^2)	T	Temperature (K)
k_t	thermal conductivity (W/m.K)	u, v	Velocity components in the x, y direction (m/s)
k	turbulent kinetic energy (m^2/s^2)	V	Volume (m^3)
L	chimney's height (m)	w	air gap (m)
P	pressure (Pa)	x,y	Cartesian coordinate (m)
Pr	Prandtl No.		

Greek Symbols			
α	absorptivity	μ_t	turbulent viscosity ($N.s/m^2$)
β	volume coefficient of expansion (1/K)	μ_{eff}	effective kinematics viscosity ($N.s/m^2$)
ε_t	emissivity	ρ	air density (kg/m^3).
ε	rate of dissipation of kinetic energy (m^2/s^2)	τ	transmisivity
η	thermal efficiency	μ	dynamic viscosity ($N.s/m^2$)